electronics

MDPI

Article

A New Flicker Detection Method for New Generation Lamps Both Robust to Fundamental Frequency Deviation and Based on the Whole Voltage Frequency Spectrum

Sıtkı Akkaya [1,2,*] and Özgül Salor [1]

1 Department of Electrical and Electronics Engineering, Faculty of Engineering, Gazi University, 06570 Maltepe Ankara, Turkey; salordurna@gazi.edu.tr

2 Department of Electrical and Electronics Engineering, Faculty of Engineering and Architecture, Bozok University, 66200 Yozgat, Turkey

* Correspondence: stk.akkaya@gmail.com; Tel.: +90-354-242-2002

Received: 3 May 2018; Accepted: 15 June 2018; Published: 19 June 2018

Abstract: A simplified Voltage Peak Detection (VPD)-based flickermeter based on spectral decomposition is proposed in this paper to detect flicker caused by high-frequency interharmonic components which effect the illumination of next-generation lamps, such as LEDs and compact fluorescent lamps. The proposed VPD-based flickermeter is specially designed to be robust to fundamental frequency deviations, which is a reality of all power systems. The proposed flickermeter is developed using a sinusoidal voltage model and it is analytically shown that flicker depends on the additive effect of the amplitudes of all the interharmonic components. Flicker results obtained by the proposed VPD-based flickermeter, IEC 61000-4-15 flickermeter, and another spectral analysis based IEC flickermeter are all compared with both synthetic voltage waveforms and field data collected from parts of the electricity transmission system with intermittent loads such as electric arc furnaces. It has been shown that only the proposed VPD-based flickermeter is sensitive to the high-frequency interharmonic components in the voltage spectrum and they are not detected by the other flickermeters. In the literature, there is no flickermeter that considers the flicker effect of the high-frequency interharmonic components and gives accurate results in cases of fundamental frequency deviations at the same time.

Keywords: flicker detection; high-frequency interharmonics; spectral decomposition; voltage peak detection (VPD); flickermeter; instantaneous flicker sensation

1. Introduction

Light flicker, being one of the fundamental power quality parameters, is caused by low-frequency voltage amplitude fluctuations. This distortion of the enlightenment caused by voltage fluctuations has an irritating effect on people, which is measured by the method recommended in the IEC (International Electrotechnical Commission) Standard 61000-4-15 [1]. However, it is known that, in its present form, the IEC flickermeter is suffering from some deficiencies [2,3].

One of these deficiencies is that the source and direction of the flicker can't be determined. Some solutions are provided in the literature [2,3]. Another problem with the IEC flickermeter is that there can be divergences in the measurements from the human perception [4,5]. Low pass filters (LPF) and Root-Mean-Square (RMS) computations are introduced to be used instead of blocks 4 and 5 of the IEC flickermeter to reduce this problem and improvement has been reported with this method in [5].

Another shortcoming of the IEC flickermeter is that it is adjusted only for the incandescent lamp [2]. However, studies show that modern lamps, such as compact fluorescents and LEDs, have different enlightenment response to fluctuating voltages [6–10], and the IEC flickermeter operates only for the incandescent lamp response. It has been emphasized that the standardized model for the incandescent lamp cannot measure the light flicker caused by other types of lamps [6]. Tests on the amount of light flicker measured from different types of lamps show that even though the flicker severity measured from the input voltage exceeds the limits, the actual light flicker caused by the LEDs are much below the limits while compact fluorescent lamps (CFLs) exceed the limits a little, but not significantly [8]. It is clearly shown that 24 different LED lamps exhibit different light intensity variations caused by the same voltage fluctuation and it is also stated that a new flicker curve is required because LED lamps cause less light intensity variation for the voltage fluctuations below 10 Hz. [9]. It has been stated that the lamps do not exhibit linear behaviors. Some have a higher voltage fluctuation amplitude than the incandescent lamps, while others have smaller. It was observed that synthetic and real voltage signals with similar fluctuation values did not give the same flicker values. For this reason, there is no guarantee that an energy saver lamp is less sensitive than incandescent lamps at every voltage fluctuation level [10]. Correcting calculation errors caused by instantaneous changes has been tried with a hybrid intelligent flicker intensity estimation method and it has been shown that the proposed method is better than other tested intelligent methods [11]. In another study, the analytical model of the IEC flickermeter was proposed, and this model was tested in the field with two different loads causing flicker in a laboratory environment and the method is reported to detect the short-term flicker severity values (P_{st}) accurately [12]. Another algorithm, which uses the fundamental frequency and harmonics to detect the flicker frequency, is presented and stated to give good P_{st} estimates on the synthetic data [13].

So far, all of the work in the literature listed above depends on the Amplitude Modulation (AM) modulated signal model for the voltage signal with flicker. However, this does not actually fit the voltage signal in the field. A large number of interharmonic components added to the fundamental and the harmonic components also cause flicker and the flicker model should be formulated as to this reality. In a study using a new model considering this phenomenon, successful P_{st} estimations are obtained [14].

In another work, it is stated that there is a relation between the 2nd harmonics and the P_{st}, but the IEC flickermeter cannot measure it since it is filtering out all high-frequency components, which is stated to be a deficiency of the IEC flickermeter [15]. In a recent study based on RMS measurement for flicker estimation, it is stated that, as the frequency increases, the ripple will decrease and therefore the VPD based flickermeter should be used [16]. It is said that, while incandescent filament lamps are sensitive to the interharmonics around the fundamental frequency, LEDs and CFLs are also sensitive to high frequency interharmonics around the odd harmonic frequencies to which incandescent lamps are insensitive [17]. LEDs and CFL lamps, which are more sensitive to VPD, in a VPD-based flickermeter proposed by [18], better flicker estimations are obtained for these lamps, which are also robust to phase-angle jumps [18]. In [19], a modified flickermeter is designed to sense the high frequency interharmonics causing the flicker, which provides more realistic results compared to the classical RMS voltage computation based methods designed for incandescent lamps [19].

Certain variable frequency drives (VFDs) are known to add interharmonics to the system, which cause voltage flicker. An interharmonic flicker curve is proposed to obtain the flicker-induced interharmonic components depending on the VPD in [20]. It has been shown that CFLs and LEDs themselves produce visible flicker by forming components around the fundamental harmonic through the rectifiers of the interharmonic components around the 3rd and 5th harmonics [21]. In [21–23], it is shown that high-frequency interharmonics for different lamps cause significant flicker and it is reported that the lamps produced should be tested in the range of 0.1 Hz and 2.5 KHz (if possible up to 9 KHz). Average, RMS, and VPD-based flickermeters are used and results are quite similar for frequency components less than 100 Hz, whereas, for larger frequencies, good results are obtained with only the VPD method [24]. A flickermeter that is recommended in [25] detects only the high-frequency interharmonic components. In another study, the VPD-based flickermeter is designed to combine individual effects of all the interharmonic components [26]. In [27], an FFT-based flickermeter robust to the fundamental frequency deviation is proposed and it is shown that the total instantaneous flicker sensation can be found as the sum of the individual instantaneous flicker sensations generated by each low-frequency interharmonic component contributing to flicker. In that work, however, high-frequency interharmonic components are not taken into consideration [27].

It is understood from all of these studies that there is a need for a flickermeter, which is designed for all types of lamps and which senses the flicker caused by the interharmonics in the entire frequency spectrum, even if there are instantaneous changes in the signal. In a previous work of the authors, a new flickermeter and a flicker curve have been proposed to meet the above shortcomings by uncovering the disadvantages of recommended flickermeters in the literature. It is also shown analytically that the light flicker should be determined not by using the AM signaling model as in the IEC flickermeter but the interharmonic signal model. It should also be noted that not only the low-frequency interharmonic components but also the high frequency interharmonic components have almost the same effect as the low frequencies. In the case of the flicker caused by the high-frequency interharmonics, VPD flickermeter detects the flicker while IEC flickermeter doesn't. Hence, a new VPD flickermeter with a new flicker curve considering also the high-frequency interharmonics is suggested in the previous work [28]. This new flickermeter is shown to detect the flicker caused by high-frequency interharmonics and to be much more robust to the fundamental frequency deviations, such as in cases of electric arc furnace loads [26,29].

In this paper, a simplified VPD flickermeter based on the spectral decomposition method in [27] is proposed using the relative amplitude in the flicker curve obtained in [28]. The maximum value of the instantaneous flicker sensitivity, S_{max}, values are obtained using 0.2 s (10 cycles of the 50 Hz fundamental frequency) windows overlapping nine cycles. Here, different S_{max} calculation methods consider the fact that interharmonic components are not evenly distributed around the fundamental and harmonics while spectral decomposition is used to detect S_{max}. After selecting the best one among these S_{max} calculation methods, flicker estimations are computed with field data obtained from a substation supplying an electric arc furnace plant.

This paper consists of seven parts. Section 2 briefly addresses the deficiencies of IEC and VPD flickermeters. In Section 3, simplification by mathematical inference for the VPD flickermeter is shown. In Section 4, the proposed simplified VPD flickermeter method is described. The results obtained using both synthetic and field data are shown in Sections 5 and 6. The results are highlighted in the last chapter.

2. Problem Definition

Deficiencies of the IEC and VPD flickermeters can be summarized as follows:

- IEC flickermeter cannot sense flicker resulting from high frequency interharmonic components.
- IEC flickermeter models the signal with flicker as an AM modulated signal, which results in evenly distributed interharmonics around the fundamental and the harmonics and this does not fit the case of actual transmission system voltage waveforms.
- IEC flickermeter usually suffers from fundamental frequency deviations, which is a fact of the electric system due to time-varying load-generation balance.
- VPD flickermeter proposed in [26], which detects high-frequency components and deems flicker as a signal with interharmonic components instead of an AM modulated signal, is incompatible with the IEC flickermeter.
- VPD flickermeter in [26] has a highly faulty response in case of fundamental frequency deviation. Hence, a new flicker curve is needed to cope with this problem.

The aim of this work is to introduce a new spectral decomposition based flicker computation method to take care of all these deficiencies.

In [27], it is shown that the instantaneous flicker sensation can be computed as the summation of the flicker effects of each individual frequency component in the voltage spectrum. In Equation (1), the effect of the ith frequency component on the instantaneous flicker sensation, where $\frac{\Delta V_i}{V}$ represents the ratio of the ith flicker frequency amplitude to the fundamental frequency component amplitude [27]:

$$S_{\max(i)} = \frac{(V^4/8)(\Delta V_i/V)^2 H(f_{B_i})^2}{(V^4/8)(\Delta V_i/V)^2{}_{IEC} H(f_{B_i})^2} = \frac{\left(\frac{\Delta V_i}{V}\right)^2}{\left(\frac{\Delta V_i}{V}\right)^2_{IEC}}. \tag{1}$$

In Equation (1), $(\frac{\Delta V_i}{V})_{IEC}$ corresponds to the $\frac{\Delta V_i}{V}$ values resulting in unity instantaneous flicker sensation at the output of Block-4 of the IEC flickermeter. $H(f_{B_i})$ is the frequency response of the filters in the IEC 61000-4-15 flickermeter at each flicker component f_{B_i}. The resultant S_{max} value according to [27] is obtained as the sum of $S_{\max(i)}$ values for all interharmonic components existing in the voltage spectrum as given in (2):

$$S_{max} = \sum_{i=1}^{N} S_{\max(i)}. \tag{2}$$

However, this computation method assumes that interharmonic frequency components are evenly distributed around the fundamental frequency. In cases of fundamental frequency deviations and highly time-varying loads such as electric arc furnaces, S_{max} computation can be varied to obtain closer values to the actual instantaneous flicker sensation values as suggested in (3)–(5):

$$S_{1\ max} = \sum_{k=1}^{(N-1)/2} \left(\frac{\sqrt{V_c[k]\ V_c[N-k+1]}}{\Delta V_{VPD(k)}/V} \right)^2, \tag{3}$$

$$S_{2\ max} = \frac{\sum_{k=1}^{N} \left(\frac{|V_c[k]|}{\Delta V_{VPD(k)}/V} \right)^2}{2}, \tag{4}$$

$$S_{3\ max} = (\sum_{k=1}^{\frac{N-1}{2}} \left(\frac{|V_c[k]| + |V_c[N-k+1]| + |V_c[-k]| + |V_c[-(N-k+1)]|}{4\ \Delta V_{VPD(k)}/V} \right)^2, \tag{5}$$

where $V_c[k]$ values are the spectral corrected amplitudes of the interharmonics formed around the fundamental frequency causing the flicker, "N" is the number of flicker components around the fundamental and $\Delta V_{VPD}/V$ are the relative amplitude values for each frequency to obtain unity instantaneous flicker sensation value for the VPD flickermeter [28]. Table 1 provides a list of $\Delta V_{VPD}/V$ values causing unity S_{max} for all interharmonic frequencies starting from 1 Hz to 25 Hz (which correspond to 50 Hz $\pm$ interharmonic frequency in the voltage frequency spectrum). $\Delta V_{VPD}/V$ values in Table 1 are half the values given in the IEC Standard 61000-4-15 since the total effect of the beat frequencies around the fundamental are listed in the standard. Here, in Table 1, effects of the individual interharmonic frequencies are listed, which is actually one of the advantages of the proposed method in this paper, i.e., different frequencies causing the same beat effect are allowed to have their own effects on the measured flicker.

If the fundamental frequency does not shift and the sampling rate is chosen to be an integer multiple of this frequency, all S_{max} values suggested in Equations (3)–(5) are equal to each other if their frequencies are in the same distance to the fundamental frequency. However, in cases of highly time-varying loads such as electric arc furnaces resulting in time-varying voltages, discrete Fourier Transform based methods cannot detect frequency components accurately. Moreover, interharmonic components of actual voltage signals are not evenly distributed around the fundamental frequency, which leads to erroneous calculations for the methods based on the modulated signal model given of the IEC flickermeter [1]. To overcome this situation, both spectral correction and different S_{max} calculation methods have been focused on and different results are obtained.

Table 1. The input relative $\Delta V_{VPD}/V$ values for each interharmonic frequency f_{IH}.

f_{IH} (Hz)	**25/75**	**26/74**	**27/73**	**28/72**	**29/71**
% $\Delta V_{VPD}/V$	0.5125	0.4777	0.4440	0.4117	0.3804
f_{IH} (Hz)	**30/70**	**31/69**	**32/68**	**33/67**	**34/66**
% $\Delta V_{VPD}/V$	0.3505	0.3216	0.2938	0.2674	0.2421
f_{IH} (Hz)	**35/65**	**36/64**	**37/63**	**38/62**	**39/61**
% $\Delta V_{VPD}/V$	0.2182	0.1957	0.1750	0.1565	0.1411
f_{IH} (Hz)	**40/60**	**41/59**	**42/58**	**43/57**	**44/56**
% $\Delta V_{VPD}/V$	0.1304	0.1247	0.1274	0.1395	0.1622
f_{IH} (Hz)	**45/55**	**46/54**	**47/53**	**48/52**	**49/51**
% $\Delta V_{VPD}/V$	0.1971	0.2476	0.3214	0.4379	0.6961

3. Simplification of VPD Flickermeter

When the flicker is expressed with the interharmonic signal model, more precise flicker detection can be performed for both the new generation lamps using rectifiers such as CFLs, LEDs, and the incandescent lamps. To achieve this, VPD flickermeter, which detects flicker using a down-up sampling method, is used [26]. Block diagram of the VPD flickermeter is shown in Figure 1a. Also the IEC 61000-4-15 flickermeter is represented in Figure 1b for comparison.

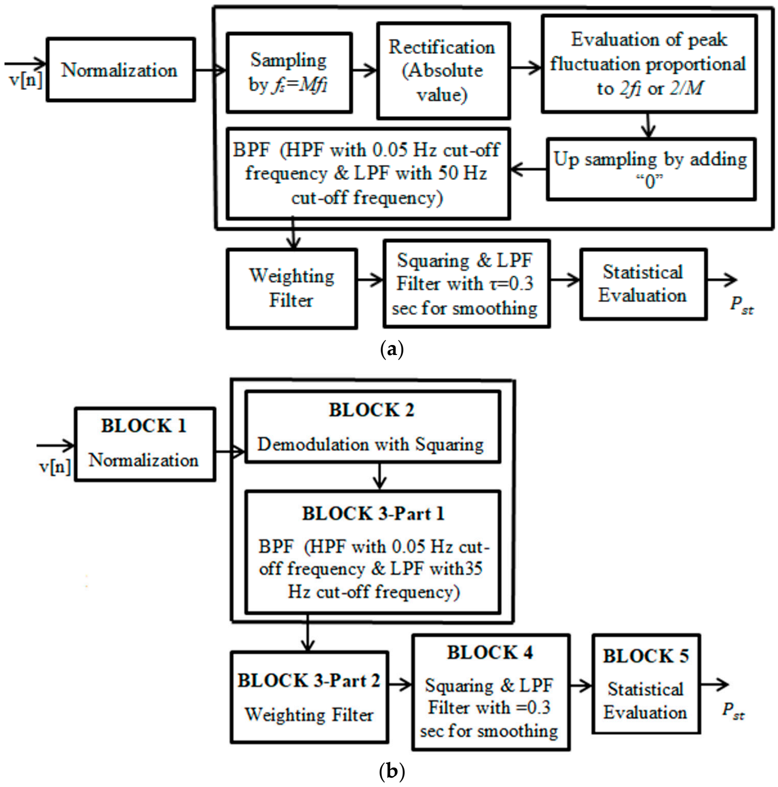

Figure 1. Block diagram of the flickermeters (**a**) Voltage Peak Detection (VPD) flickermeter proposed in [26]; (**b**) IEC 61000-4-15 flickermeter in [1].

In the VPD flickermeter illustrated in Figure 1a, block 2 and block 3 of the IEC flickermeter recommended in [1], as in Figure 1b, are changed [26]. Instead of these blocks, sampling is achieved with the sampling frequency $f_s = Mf_1$ and M is an integer such that f_s is an integer multiple of the fundamental frequency f_1. Then, a "rectification" is applied that is mathematically taking the "absolute value". Peak voltage is then obtained by "down sampling" by $2f_1$ or $2/M$. When the peak point is determined, "up sampling" is performed by f_s, keeping the two peaks inside one cycle and replacing all other samples by zeros. As the last step, a low-pass filter (LPF), with cut-off frequencies of 50 and 60 Hz for 50 and 60 Hz systems, is used in this flickermeter, while the IEC 61000-4-15 flickermeter uses these of 35 and 42 Hz, respectively. The rest of the system is the same as the IEC flickermeter [26]. In addition, a high pass filter (HPF) with cut-off frequencies of 0.05 Hz is used in this flickermeter. LPF and HPF flickermeter constitutes band pass filter (BPF). The rest of the flickermeter is the same as IEC 61000-4-15 flickermeter.

New generation lamps such as LEDs and CFLs are more susceptible to peak amplitude fluctuation and therefore the VPD flickermeter method is preferred when they are used. This is because these lamps, excluding the incandescent lamps, carry the high-frequency interharmonic components to the interharmonic frequencies around the fundamental and the odd harmonic due to their operation principles.

The signal with flicker is modeled as in (6) using the interharmonic signal model:

$$v(t) = V\left[\sin(2\pi f_1 t) + \frac{\Delta V}{V}\sin(2\pi f_{IH} t + \varnothing_{IH})\right] f_h = h f_1\ f_B = |f_{IH} - f_h|. \tag{6}$$

"V" in (6) symbolises the system amplitude, f_1 is the fundamental frequency, $\frac{\Delta V}{V}$ is relative the amplitude of the interharmonic signal, f_{IH} is the frequency of this interharmonic, "h" is an odd number, f_h is the odd harmonic, f_B is the flicker frequency of the interharmonic and f_{IH} represents the component of the flicker.

Equation in (6) can be rewritten as in (7):

$$v(t) = V\left[\begin{array}{c}\sin(2\pi f_1 t)\\ +\\ \frac{\Delta V}{V}(\cos(2\pi(f_B)t + \varnothing_{IH})\sin(2\pi(hf_1)t) + \sin(2\pi(f_B)t + \varnothing_{IH})\cos(2\pi(hf_1)t))\end{array}\right]. \tag{7}$$

If $v(t)$ is defined as the input signal in Figure 1a, then the rectified signal in Figure 1a (output of Rectification block) can be expressed as a square wave function multiplied by the sinusoidal expression [26]. Square wave $s(t)$ is given as in (8) using the Taylor series expansion:

$$s(t) = \frac{4}{\pi}\sum\nolimits_{n=1,3\ldots}\frac{1}{n}\sin(2\pi n f_1 t). \tag{8}$$

Hence, a rectified form of $v(t)$ or $|v(t)|$ can be expressed as given in (9):

$$\begin{aligned}|v(t)| = v(t)s(t) &= \left(\sin(2\pi f_1 t) + \tfrac{\Delta V}{V}\sin(2\pi f_{IH} t + \varnothing_{IH})\right)\left(\tfrac{4}{\pi}\sum_{n=1,3\ldots}\tfrac{1}{n}\sin(2\pi n f_1 t)\right)\\ &= \left\{\tfrac{4}{\pi}\sum_{n=1,3\ldots}\tfrac{1}{n}\sin(2\pi f_1 t)\sin(2\pi n f_1 t) + \tfrac{4}{\pi}\sum_{n=1,3\ldots}\tfrac{1}{n}\tfrac{\Delta V}{V}\sin(2\pi f_{IH} t + \varnothing_{IH})\sin(2\pi n f_1 t)\right\}\\ &= \left\{\begin{array}{c}\langle\tfrac{4}{\pi}\sum_{n=1,3\ldots}\tfrac{1}{2n}\cos(2\pi(n-1)f_1 t) - \tfrac{1}{2n}\cos(2\pi(n+1)f_1 t)\rangle\\ +\\ \langle\tfrac{4}{\pi}\sum_{n=1,3\ldots}\tfrac{1}{2n}\tfrac{\Delta V}{V}\cos(2\pi(f_{IH} - nf_1)t + \varnothing_{IH}) - \tfrac{1}{2n}\tfrac{\Delta V}{V}\cos(2\pi(f_{IH} + nf_1)t + \varnothing_{IH})\rangle\end{array}\right\}.\end{aligned} \tag{9}$$

The final equations in (10) and (11), the first part of (9) with the singular harmonics $v_f(t)$, and the second part of it with the interharmonics as $v_{IH}(t)$, are, respectively:

$$v_f(t) = \frac{4}{\pi}\sum_{n=1,3\ldots}\frac{1}{2n}\cos(2\pi(n-1)f_1 t) - \frac{1}{2n}\cos(2\pi(n+1)f_1 t)\ , \tag{10}$$

$$v_{IH}(t) = \frac{4}{\pi}\sum\nolimits_{n=1,3\ldots}\frac{1}{2n}\frac{\Delta V}{V}\cos(2\pi(f_{IH}-nf_1)t+\varnothing_{IH}) - \frac{1}{2n}\frac{\Delta V}{V}\cos(2\pi(f_{IH}+nf_1)t+\varnothing_{IH})\,. \quad (11)$$

Equations (10) and (11) are expressed as discrete time signals $v_f[k]$ and $v_{IH}[k]$ in (12) and (13), respectively:

$$\begin{aligned} v_f[k] &= v_f\left(t_0+\tfrac{k}{2f_1}\right), \\ &= V\tfrac{2}{\pi}\sum_{n=1,3\ldots}\tfrac{1}{n}\left\{\cos\left(2\pi(n-1)f_1\left(t_0+\tfrac{k}{2f_1}\right)\right)-\cos\left(2\pi(n+1)f_1\left(t_0+\tfrac{k}{2f_1}\right)\right)\right\} \\ &= \langle V\tfrac{2}{\pi}\sum\nolimits_{n=1,3\ldots}\tfrac{1}{n}\left\{\begin{array}{c}\cos(2\pi(n-1)f_1t_0+(n-1)\pi k)\\ -\cos(2\pi(n+1)f_1t_0+(n+1)\pi k)\end{array}\right\}\rangle, \end{aligned} \quad (12)$$

$$\begin{aligned} v_{IH}[k] &= v_{IH}\left(t_0+\tfrac{k}{2f_1}\right), \\ &= \mathrm{V}\tfrac{2}{\pi}\tfrac{\Delta V}{V}\sum_{n=1,3\ldots}\tfrac{1}{n}\left\{\begin{array}{c}\cos\left(2\pi((hf_1\pm f_B)-nf_1)\left(t_0+\tfrac{k}{2f_1}\right)+\varnothing_{IH}\right)\\ -\cos\left(2\pi((hf_1\pm f_B)+nf_1)\left(t_0+\tfrac{k}{2f_1}\right)+\varnothing_{IH}\right)\end{array}\right\} \\ &= V\tfrac{2}{\pi}\tfrac{\Delta V}{V}\sum\nolimits_{n=1,3\ldots}\tfrac{1}{n}\left\{\cos\left(2\pi l_{f_B}\mathrm{k}+\varnothing_{IH}^{n^-}\right)-\cos\left(2\pi l_{f_B}\mathrm{k}+\varnothing_{IH}^{n^+}\right)\right\}. \end{aligned} \quad (13)$$

In (12) and (13), "k" is the discrete time index, t_0 is the first sampling time; (L = 0, 1, 2, ...), where $2\pi(n-1)f_1t_0$ is independent of the semantic value k and $(n\pm1)\pi k$ is $2l\pi k(l=0,\ 1,\ 2,\ldots)$ because of an odd integer notation "n", and thus $v_f[k]$ value is obtained as the "DC" term.

$f_{IH}=hf_1\pm f_B$ ($h=2p+1$, $p=0,1,2,3,\ldots$) and $t_0=1/4f_1$ (due to peak detection at each quarter period of the fundamental) are expressed in (13) and the variables are given as follows:

$$\varnothing_{IH}^{n^-} = 2\pi((h-n)f_1\pm f_B)t_0+(h-n)\pi k+\varnothing_{IH}\,, \quad (14)$$

$$\varnothing_{IH}^{n^+} = 2\pi((h+n)f_1\pm f_B)t_0+(h+n)\pi k+\varnothing_{IH}, \quad (15)$$

$$l_{f_1} = \pm\frac{f_B}{2f_1}\,. \quad (16)$$

$|v(t)|$ expression will then be passed through the Band Pass Filter (BPF) and Low Pass Filter (LPF), so that the high frequency components and the DC term will be filtered and, as a result, final expression will be as given in (17):

$$\begin{aligned} |v[k]| &\approx V\tfrac{2}{\pi}\tfrac{\Delta V}{V}\sum\nolimits_{n=1,3\ldots}\tfrac{1}{n}\left\{\cos\left(2\pi l_{f_B}\mathrm{k}+\varnothing_{IH}^{n^-}\right)\right\}, \\ &= V\tfrac{2}{\pi}\tfrac{\Delta V}{V}\sum\nolimits_{n=1,3\ldots}\tfrac{1}{n}\left\{\begin{array}{c}\cos\left((2\pi(hf_1\pm f_B)-nf_1)\left(t_0+\tfrac{k}{2f_1}\right)+\varnothing_{IH}\right)\\ -\cos\left((2\pi(hf_1\pm f_B)+nf_1)\left(t_0+\tfrac{k}{2f_1}\right)+\varnothing_{IH}\right)\end{array}\right\}. \end{aligned} \quad (17)$$

If the first *cosine* expression in (17) is explicitly rewritten, (18) is obtained.

$$\cos(a\mp b) = \cos\left(2\pi((h-nf_1)t_0)+(h-n)\pi k\mp 2\pi f_B\left(t_0+\frac{k}{2f_1}\right)+\varnothing_{IH}\right). \quad (18)$$

The $\varnothing_{IH}$ phase value in this equation is neglected and then the cosine term in (18) can be written as in (20) using the trigonometric identity given in (19):

$$\cos(a\mp b) = \cos(a)\cos(b)\pm\sin(a)\sin(b). \quad (19)$$

If it is used according to the Equation (18), it will be like (20):

$$\cos(a \mp b) = \left\{ \begin{array}{c} \cos[2\pi(h-n)f_1)t_0 + (h-n)\pi k] \cos\left[2\pi f_B\left(t_0 + \frac{k}{2f_1}\right)\right] \\ \pm \\ \sin\left[2\pi(h-n)f_1)t_0 + (h-n)\pi k\right] \sin[2\pi f_B\left(t_0 + \frac{k}{2f_1}\right)\right] \end{array} \right\}. \tag{20}$$

Furthermore, if $t_0 = T_1/4$ is substituted in the expression, *cosine* expression in (21) is obtained because $T_1 = 1/f_1$:

$$\cos(a \mp b) = \left\{ \begin{array}{c} \cos\left[2\pi\left(\frac{(h-n)}{4}\right) + (h-n)\pi k\right] \cos\left[2\pi f_B\left(\frac{1}{4f_1} + \frac{k}{2f_1}\right)\right] \\ \pm \\ \sin\left[2\pi\left(\frac{(h-n)}{4}\right) + (h-n)\pi k\right] \sin[2\pi f_B\left(\frac{1}{4f_1} + \frac{k}{2f_1}\right)\right] \end{array} \right\}. \tag{21}$$

When $h = 1, 3, 5, \ldots$ and $n = 1, 3, 5, \ldots$. $(h - n)$ *is* even and cosine and sine components with $(h - n)\pi$ terms cancel out and denoting them by A_1 and B_1 respectively, (22) is obtained:

$$\cos(a \mp b) = A_1 \ \cos\left[2\pi f_B\left(\frac{1}{4f_1} + \frac{k}{2f_1}\right)\right] \pm B_1 \ \sin\left[2\pi f_B\left(\frac{1}{4f_1} + \frac{k}{2f_1}\right)\right]. \tag{22}$$

It is obvious that $B_1 = 0$ for all values of even $(h - n)$, so that the left side of the expression " $\pm$ " is equal to zero. The expression A_1 will be as given in (23) depending on the value of $(h - n)$*:*

$$\begin{array}{ll} (h-n) = \ldots - 8, -4, 0, 4, 8, \ldots; & A_1 = 1 \\ (h-n) = \ldots - 10, -6, -2, 2, 6, 10; & A_1 = -1 \end{array} \tag{23}$$

Due to (23), (22) can be expressed as given in (24):

$$\cos(a \mp b) = A_1 \cos\left(2\pi f_B\left(1/4f_1 + \frac{k}{2f_1}\right)\right). \tag{24}$$

Similarly, the second cosine expression in (17) can be explicitly written as in (25):

$$\cos(c \mp d) = \ \cos\left(2\pi(h + nf_1)t_0 + (h+n)\pi k \mp 2\pi f_B\left(t_0 + \frac{k}{2f_1}\right) + \varnothing_{IH}\right). \tag{25}$$

If $\varnothing_{IH}$ is omitted and the expression (25) is derived according to (19), (26) is obtained:

$$\cos(c \mp d) = \left\{ \begin{array}{c} \cos[2\pi\left((h+n)f_1\right)t_0 + (h+n)\pi k] \cos[2\pi f_B\left(t_0 + \frac{k}{2f_1}\right)\right] \\ \pm \\ \sin[2\pi\left((h+n)f_1\right)t_0 + (h+n)\pi k] \sin[2\pi f_B\left(t_0 + \frac{k}{2f_1}\right)\right] \end{array} \right\}. \tag{26}$$

Furthermore, if $t_0 = T_1/4$ is substituted in the expression, this *cosine* expression is obtained as given in (27), since $T_1 = 1/f_1$:

$$\cos(c \mp d) = \left\{ \begin{array}{c} \cos\left[2\pi\left(\frac{(h+n)}{4}\right) + (h+n)\pi k\right] \cos\left[2\pi f_B\left(\frac{1}{4f_1} + \frac{k}{2f_1}\right)\right] \\ \pm \\ \sin\left[2\pi\left(\frac{(h+n)}{4}\right) + (h+n)\pi k\right] \sin\left[2\pi f_B\left(\frac{1}{4f_1} + \frac{k}{2f_1}\right)\right] \end{array} \right\}. \tag{27}$$

When h = *1, 3, 5, . . .* and n = *1, 3, 5, ...*, $(h - n)$ is even and cosine and sine components with $(h - n)\pi$ terms cancel out and denoting them by A_2 and B_2, respectively, as (28):

$$\cos(c \mp d) = A_2 \cos\left[2\pi f_B\left(\frac{1}{4f_1} + \frac{k}{2f_1}\right)\right] \pm B_2 \sin\left[2\pi f_B\left(\frac{1}{4f_1} + \frac{k}{2f_1}\right)\right]. \tag{28}$$

It is clear that B_2 = 0 for all values of $(h + n)$, so that the left side of the expression " $\pm$ " becomes zero. A_2 is expressed as in (29) according to the values of $(h + n)$:

$$\begin{array}{ll} (h+n) = 2, 6, 10, \ldots; & A_2 = -1, \\ (h+n) = 4, 8, 12; \ldots, & A_2 = 1. \end{array} \tag{29}$$

Then, the expression in (28) can be written as given in (30). In addition, using the expressions (23) and (24), $|v[k]|$ can be written as in (31):

$$\cos(a \mp b) = A_2 \cos\left(2\pi f_B\left(1/4f_1 + \frac{k}{2f_1}\right)\right). \tag{30}$$

Considering the expressions (23) and (29), the changes of the expressions A_1 and A_2 will be examined as in (32) assuming that $h = 1$ and $n = 1,\ 3,\ 5,\ 7,\ 9,\ \ldots$, respectively. Note that only the components around the fundamental frequency exist in Equation (31). In this equation, $H(f_B)$ is the frequency response of the flicker frequency component of the filters in the IEC 61000-4-15 flickermeter:

$$|v[k]| \approx V\frac{2}{\pi}\frac{\Delta V}{V}\sum_{n=1,3\ldots}^{\infty}\frac{(A_1 - A_2)}{n}\cos\left(2\pi f_B\left(\frac{1}{4f_1} + \frac{k}{2f_1}\right)\right)H(f_B), \tag{31}$$

$$\begin{array}{ll} \text{if } n = 1 \text{ and } h = 1, \text{ then } A_1 = 1,\ A_2 = -1 & \text{and } A_1 - A_2 = 2 \\ \text{if } n = 3 \text{ and } h = 1, \text{ then } A_1 = -1,\ A_2 = 1 & \text{and } A_1 - A_2 = -2 \\ \text{if } n = 5 \text{ and } h = 1, \text{ then } A_1 = 1,\ A_2 = -1 & \text{and } A_1 - A_2 = 2 \\ \text{if } n = 7 \text{ and } h = 1, \text{ then } A_1 = -1,\ A_2 = 1 & \text{and } A_1 - A_2 = -2 \\ \text{if } n = 9 \text{ and } h = 1, \text{ then } A_1 = 1,\ A_2 = -1 & \text{and } A_1 - A_2 = 2 \end{array} \tag{32}$$

Therefore, Equation (31) can be expressed as in (33):

$$|v[k]| \approx V\frac{2}{\pi}\frac{\Delta V}{V}\sum\nolimits_{n=1,3\ldots}^{\infty}\frac{2}{n}(-1)^{\frac{(n-1)}{2}}\cos\left(2\pi f_B\left(\frac{1}{4f_1} + \frac{k}{2f_1}\right)\right)H(f_B). \tag{33}$$

It is obvious that this expression is independent of the "n" value and has positive and negative values, respectively, as given in (32).

If the statement in (33) is written again as in (31), then (34) follows:

$$|v[k]| \approx V\frac{2}{\pi}\frac{\Delta V}{V}\ \cos\left(2\pi f_B\left(\frac{1}{4f_1} + \frac{k}{2f_1}\right)\right)\ H(f_B)\ \sum_{n=1,3\ldots}^{\infty}\frac{2}{n}\ (-1)^{\frac{(n-1)}{2}}. \tag{34}$$

The end part of the total expression in (34) can be approximated as in (35):

$$\sum_{n=1,3}^{\infty}\frac{2}{n}(-1)^{\frac{(n-1)}{2}} \approx \frac{\pi}{4}\ . \tag{35}$$

Therefore, when the expression in (35) is substituted in (34), (36) is obtained:

$$|v[k]| \approx V\frac{\Delta V}{V}\cos\left(2\pi f_B\left(\frac{1}{4f_1} + \frac{k}{2f_1}\right)\right)H(f_B). \tag{36}$$

This expression shows the output of the weighting filter following BPF (HPF with 0.05 Hz cut-off frequency + LPF with 50 Hz cut-off frequency) in Figure 1a. When the square of the expression in (36) is taken, it can be shown as in (37):

$$|v[k]|^2 \approx V^2 \frac{\Delta V}{V^2}^2 \frac{1}{2}\left\{1+\cos\left(2\pi 2 f_B\left(\frac{1}{4f_1}+\frac{k}{2f_1}\right)\right)\right\} H^2(f_B). \tag{37}$$

The $2f_B$ frequency component constituting the fluctuation is passed through the last LPF with a time constant of $\tau = 0.3$ s as recommended in the IEC Standard [1] to obtain the instantaneous flicker sensation S_{max} value in (38) [27]:

$$S_{max} \approx \frac{\Delta V}{V^2}^2 \frac{1}{2} H^2(f_B)\,. \tag{38}$$

$H(f_B)$ in (38) is the frequency response of all the filters in the VPD flickermeter at the frequency $f_B = |f_{IH} - f_h|$. The $|v[k]|$, $|v[k]|^2$, S_{max} expressions in (36)–(38) are obtained for a signal with a single interharmonic component causing flicker. As stated in [27], there is more than one flicker component in the actual case of a power network. (38) can be expressed as the summation of the different frequency components causing the flicker as expressed in (39):

$$|u[k]| \approx V \sum_{i=1}^{N} \frac{\Delta V_i}{V} \cos\left(2\pi f_{B_i}\left(\frac{1}{4f_1}+\frac{k}{2f_1}\right)\right) H(f_{B_i}). \tag{39}$$

The expression in (39) shows the output of BPF in Figure 1a. When the square of (39) is taken, $|u[k]|^2$ can be written as in (40):

$$|u[k]|^2 \approx \left\{ \begin{array}{c} V^2 \sum_{i=1}^{N} \frac{\Delta V_i^2}{V^2} \frac{1}{2}\left\{1+\cos\left(2\pi 2 f_{B_i}\left(\frac{1}{4f_1}+\frac{k}{2f_1}\right)\right)\right\} H^2(f_{B_i}) + \\ V^2 2 \sum_{i=1}^{N} \sum_{j=i+1}^{N} \frac{\Delta V_i}{V}\frac{\Delta V_j}{V} \left[\begin{array}{c} \cos\left(2\pi\left(f_{B_i}-f_{B_j}\right)\left(\frac{1}{4f_1}+\frac{k}{2f_1}\right)\right)) H\left(f_{B_i}-f_{B_j}\right) \\ +\cos\left(2\pi\left(f_{B_i}+f_{B_j}\right)\left(\frac{1}{4f_1}+\frac{k}{2f_1}\right)\right)) H\left(f_{B_i}+f_{B_j}\right) \end{array} \right] \end{array} \right\}. \tag{40}$$

In Equation (40), components with the frequency "$2f_B$", "$f_{B_i} - f_{B_j}$", and "$f_{B_i} + f_{B_j}$" constitute the double-frequency components, the frequency-difference components and the frequency-summation components, respectively. As stated in [27], if these components are negligible, the expression in (40) can be written as in (41):

$$|u[k]|^2 \approx V^2 \sum_{i=1}^{N} \frac{\Delta V_i^2}{V^2} \frac{1}{2} H^2(f_{B_i}). \tag{41}$$

The S_{max} value, which is the value of the instantaneous flicker sensation, is obtained by passing through the last LPF with a time constant of $\tau = 0.3$ s as in (42) [1]:

$$S_{max} \approx V^2 \sum_{i=1}^{N} \frac{\Delta V_i^2}{V^2} \frac{1}{2} H^2(f_{B_i})\,. \tag{42}$$

In (42), N is the number of components to be calculated at frequencies to $f \pm 25$ Hz around the fundamental frequency. Note that the beat frequencies around the odd harmonics are reflected to the interharmonics around the fundamental by using the VPD flickermeter, hence they are already taken care of.

Based on the values of $\Delta V_{VPD}/V$ given in Table 1 and the Equation (1), individual effect of each interharmonic component ($S_{max(i)}$) is computed as in (43), using the VPD flickermeter values in Table 1:

$$S_{\max(i)} = \frac{(V^2/2)(\Delta V_i/V)^2 H(f_{B_i})^2}{(V^2/2)(\Delta V_i/V)^2{}_{VPD} H(f_{B_i})^2} = \frac{(\Delta V_i/V)^2}{(\Delta V_i/V)^2{}_{VPD}}. \tag{43}$$

The overall S_{max} value is then given as the sum of each $S_{\max(i)}$ value as in (44):

$$S_{max} \approx \sum_{i=1}^{N} S_{\max(i)}. \tag{44}$$

Hence, it can be concluded that the proposed flickermeter has lower computational complexity compared to the VPD flickermeter based on (43) and (44).

4. Proposed Simplified VPD Flickermeter Method

The block diagram of the proposed VPD-flickermeter, including the spectral verification scheme used, is given in Figure 2. In the proposed method, a comb filter is first applied on the input signal $v[k]$, to extract the fundamental frequency with the interharmonics in the neighborhood of $\pm$ 25 Hz and only the interharmonics around the odd harmonics, but not the harmonics themselves. Comb filter is obtained by using LPF, HPF and notch filter groups in parallel, specifically HPF and LPF filters with $f_h - 25$ Hz ve $f_h + 25$ Hz cut-off frequencies, and notch filters with stop frequency "f_h" at harmonics, respectively. Zero-crossing detection is applied on the filtered signal, and both the fundamental frequency "f_f" and the starting sample "n_0", which corresponds to a zero-crossing, for the DFT and the exact start time "t_0" for generating synthetic signal are determined [27,29,30]. (45) is obtained with the help of (34) to find the rectified signal with the determined starting point and the starting time:

$$v_1[k] = v[k+n_0] \sum_{n=1,3,5}^{M} \sin\left(2\pi f_f n t_{new}\right)(-1)^{(n-1)/2}, \tag{45}$$

where $v[k+n_0]$: starting from n_0 points and k runs from *0* to $N-1$, and $N = f_s * window\ length = 640$ samples. Window length is selected as 0.2 s. The other variables in (45) are listed below:

$t\_new = \mathrm{t}_0\!: \frac{1}{f_s} : 0.2 + \mathrm{t}_0$ (sample points of the signal starting at the exact zero-crossing),
n: harmonic grade,
M: number of harmonics up to $f_s/2$,
f_f: fundamental frequency.

$v_1[k]$ indicates the rectified signal. If the expression $v[k+n_0]$ is a signal at (6) starting at the point "n_0" and in the case of frequency deviation, this approach will yield erroneous results and the synthetic waveform in $v_2[k]$ is generated to compensate for the error.

In (46), the "A" value in the expression $A\sin\left(2\pi f_f t_{new}\right)$ is the actual amplitude of the fundamental component for each window and is obtained by using the DFT and it is used to obtain the amplitude of the synthetically generated signal [30]. t_{new} is used as the corrected starting point to prevent any spectral leakage due to fundamental frequency deviations:

$$v_2[k] = A\sin\left(2\pi f_f t_{new}\right) \sum_{n=1,3,5}^{M} \sin\left(2\pi f_f n t_{new}\right)(-1)^{\frac{n-1}{2}}. \tag{46}$$

In order to obtain the interharmonic components around both the fundamental frequency and the other harmonics, $Vc\,[k]$ is obtained in the frequency domain by subtracting the DFTs of signals v_1 and v_2 from each other [30]:

$$V_c[k] = \frac{V_1[k] - V_2[k]}{A}. \tag{47}$$

Due to the rectification process in (9), if there is a component around an odd harmonic, it is collected around the fundamental frequency. It should be noted that, unlike the DFT-based flickermeter proposed in [27], the flicker component here is shifted to the spectrum at 0–25 and 75–100 Hz. For example, if there is an interharmonic component of 60 Hz, it will form a component at $|50 - 60| = 10$

Hz and ∣150 − 60∣ = 90 Hz originating from the multiplication with the 3rd harmonic. The flicker frequency of this component will be at ∣n*50 − 60∣=10 Hz when n = 1 is selected, as mentioned earlier.

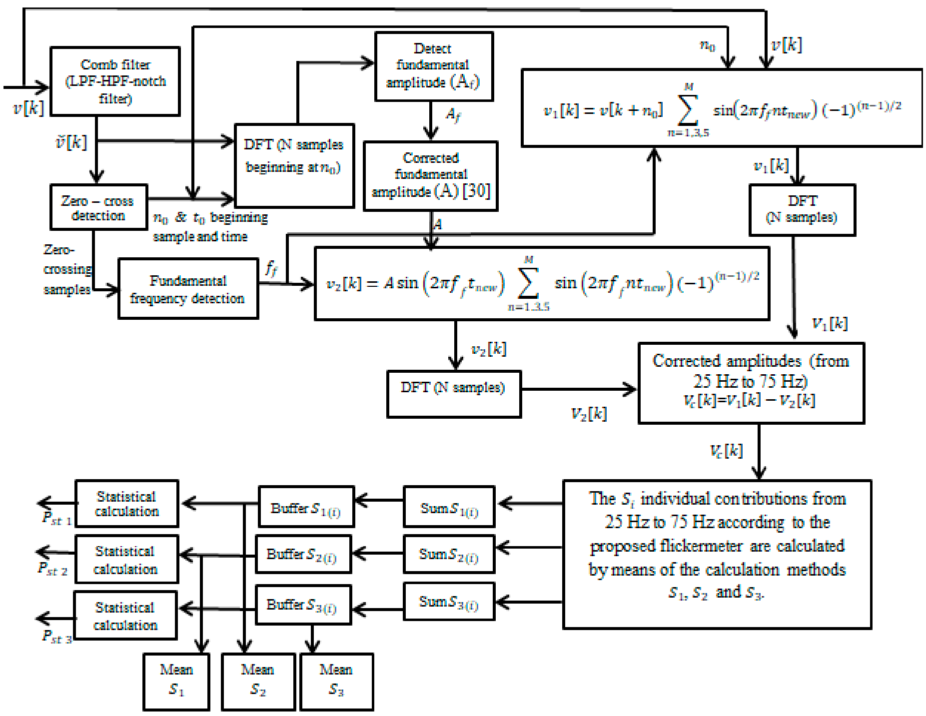

Figure 2. Block diagram of the proposed flickermeter for new generation lamps based on improved spectral decomposition approach.

Next, by taking the components from 5 to 25 Hz and 75 to 95 Hz and replacing the IEC $\frac{\Delta V}{V}$ expression in (1) with the VPD $\frac{\Delta V}{V}$ value in Table 1, the instantaneous flicker sensation values of each flicker component are obtained for the three methods (S_1, S_2, and S_3) and then $mean\_S_{max}$ and P_{st} values are computed.

It is expected that these S_{max} values will be equal to each other if the fundamental frequency does not deviate and a good sampling is performed with integer multiples of this frequency. However, since the flicker components occur with highly time-varying characteristics, the DFT components are not identically distributed at two sides of the fundamental frequency component, which leads to erroneous calculations. To overcome this problem, both spectral correction and different S_{max} calculation methods are considered and the results are compared. It has been shown that the best results are obtained with the S_1 method.

5. Results with Synthetically Generated Data

Results presented in this section have been obtained on the synthetically generated voltage waveform with interharmonics to test the accuracy of the proposed approach and also the compatibility with the IEC flickermeter standard [1].

5.1. Comparison of S_1, S_2 and S_3 Instantaneous Flicker Sensation Computation Methods in Case of Fundamental Frequency Deviation

5.1.1. Comparison of S_1, S_2 and S_3 in Case of Frequency Deviation for Low-Frequency interharmonics (around the Fundamental)

For this test, interharmonic at 40 Hz (f_{IH} = 40 Hz) is used in addition to the fundamental frequency. Furthermore, 40 Hz means a flicker frequency of 10 Hz (f_B = 10 Hz) that is closest to 8.8 Hz in case of 5 Hz resolution. In addition, 8.8 Hz is reported as the frequency for which human beings are most sensitive to the IEC flickermeter standard [1]. The study is carried out in accordance with the signal model given in (6). In that case, according to the standard, $\frac{\Delta V}{V} = 0.1304$ and it is expected that $S_{max} = 1$, $P_{st} = 0.7146$. However, as mentioned before, erroneous results are obtained when the fundamental frequency deviates, and this problem still exists even if the frequency deviation occurs inside very short time intervals. Therefore, to increase the time-resolution of the analysis, 10-min synthetic data sampled at 3200 Hz is analyzed using 10-cycle windows overlapping nine cycles. The results are given in Table 2 for S_1, S_2 *and* S_3 are the mean values of those 3000 instantaneous flicker sensation values (S) in the 10-min data.

Table 2. $mean\_S_{max}$ and P_{st} values for proposed flickermeter with 40 Hz interharmonic.

		Without Spectral Correction		**With Spectral Correction**	
	f_{line}.Hz	**$mean\_S_{max}$**	**P_{st}**	**$mean\_S_{max}$**	**P_{st}**
$mean\_S_{max}$ and P_{st} values for proposed flickermeter in case S_1	**49.5**	1435.47	27.6497	1	0.7395
	49.6	1018.21	23.3422	1	0.7340
	49.7	615.63	18.2586	1	0.7295
	49.8	286.19	12.5649	1	0.7244
	49.9	73.57	6.5048	1	0.7192
	50	1.06	0.755	1	0.7139
	50.1	69.82	6.3928	1	0.7183
	50.2	257.99	12.1171	1	0.7226
	50.3	526.82	17.2908	1	0.7271
	50.4	826.73	21.6523	0.99	0.7312
	50.5	1104.07	25.146	0.99	0.7360
$mean\_S_{max}$ and P_{st} values for proposed flickermeter in case S_2	**49.5**	10207.46	72.5229	1.01	0.7415
	49.6	6402.51	57.5226	1.01	0.7354
	49.7	3503.22	42.6595	1	0.7303
	49.8	1501.56	28.0523	1	0.7248
	49.9	359.27	13.8829	1	0.7193
	50	1.08	0.7701	1	0.7139
	50.1	317.28	13.0593	1	0.7183
	50.2	1168.95	24.8143	1	0.7228
	50.3	2398.03	35.4532	1	0.7274
	50.4	3839.47	44.8085	1	0.732
	50.5	5334.93	52.7979	1	0.737
$mean\_S_{max}$ and P_{st} values for proposed flickermeter in case S_3	**49.5**	5812.78	54.6971	1.01	0.7405
	49.6	3704.14	43.7038	1	0.7346
	49.7	2055.61	32.6215	1	0.7299
	49.8	892.07	21.5496	1	0.7246
	49.9	215.95	10.6651	1	0.7192
	50	1.07	0.7625	1	0.7139
	50.1	193.09	10.0985	1	0.7183
	50.2	711.71	19.3456	1	0.7227
	50.3	1458.76	27.7245	1	0.7272
	50.4	2327.24	35.0439	1	0.7316
	50.5	3211.47	41.2288	1	0.7365

As shown in Table 2, for each fundamental frequency value between 49.5 Hz and 50.5 Hz, calculations have been made separately. It is obvious that the $mean\_S_{max}$ and P_{st} values change too much as the distance from the fundamental frequency of 50 Hz increases, when the spectral correction is not performed, that is, the interharmonic calculation is performed directly on $V_1[k]$ instead of the operation (26). With the spectral correction, it is observed that the maximum error in $mean\_S_{max}$ is 1%. When methods S_1, S_2 *and* S_3 (i.e., (3)–(5), respectively) are compared, the method S_1 presents better results in terms of P_{st}, whether spectral correction is performed or not.

5.1.2. Comparison of S_1, S_2 and S_3 According to Frequency Deviation for High-Frequency Interharmonics

Comparison studied for the low-frequency interharmonic at 40 Hz in the previous subsection is carried out for f_{IH} = 940 Hz (f_B = 10 Hz) in this case.

The results are compatible with the low-frequency results as shown in Table 3. It is shown by this test that the proposed flickermeter is sensitive to high-frequency interharmonics, while, in the classical approach, the effect those interharmonics had would be completely eliminated.

Table 3. $mean\_S_{max}$ and P_{st} values for proposed flickermeter with 940 Hz interharmonic.

		Without Spectral Correction		With Spectral Correction	
	f_{line},Hz	$mean\_S_{max}$	P_{st}	$mean\_S_{max}$	P_{st}
$mean\_S_{max}$ **and P_{st} values for proposed flickermeter in case** S_1	**49.5**	1434.27	27.6491	1	0.725
	49.6	1017.24	23.3766	1.04	0.7496
	49.7	615.4	18.337	0.99	0.7238
	49.8	285.86	12.5912	0.99	0.7155
	49.9	73.49	6.5488	1.01	0.7221
	50	0.96	0.7135	1	0.7139
	50.1	69.94	6.4099	1.01	0.7197
	50.2	258.24	12.1578	0.99	0.7222
	50.3	527.29	17.357	1	0.7251
	50.4	826.12	21.6759	1.04	0.7419
	50.5	1104.29	25.1828	1	0.7441
$mean\_S_{max}$ **and P_{st} values for proposed flickermeter in case** S_2	**49.5**	10,208.95	72.3831	1	0.7258
	49.6	6403.70	57.3568	1.04	0.7511
	49.7	3503.35	42.3977	0.99	0.724
	49.8	1501.85	27.9419	0.99	0.7155
	49.9	359.35	13.8023	1.01	0.7222
	50	0.98	0.7196	1	0.7139
	50.1	317.16	13.0289	1.01	0.7198
	50.2	1168.78	24.8163	0.99	0.7223
	50.3	2397.7	35.3781	1	0.7252
	50.4	3838.01	44.7974	1.04	0.743
	50.5	5335	52.8165	1	0.7453
$mean\_S_{max}$ **and P_{st} values for proposed flickermeter in case** S_3	**49.5**	5812.93	54.6332	1	0.7253
	49.6	3704.25	43.6302	1.04	0.7504
	49.7	2055.56	32.5756	0.99	0.7239
	49.8	892.05	21.4719	0.99	0.7155
	49.9	215.95	10.6631	1.01	0.7221
	50	0.97	0.7161	1	0.7139
	50.1	193.09	10.0761	1.01	0.7198
	50.2	711.75	19.3879	0.99	0.7222
	50.3	1458.83	27.7466	1	0.7252
	50.4	2326.21	35.0489	1.04	0.7424
	50.5	3211.62	41.2495	1	0.7446

The same comparison for S calculation methods S_1, S_2 and S_3 also apply to this case. Almost the same results are obtained for all methods. Therefore, from now on, studies are continued using the method S_1.

5.2. Proposed Flickermeter Responses to Various Sinusoidal Voltage Fluctuations with Different Frequency Resolutions

The $mean\_S_{max}$ response of interharmonic signal model in (6) has been investigated with 5 Hz (window of 0.2 s) and 0.5 Hz (window of 2 s) resolutions when the $\frac{\Delta V}{V}$ relative amplitude values corresponding to various frequencies given in Table 4 are applied. Both low frequency and high frequency interharmonic components corresponding to the same beat frequencies are applied as shown in Table 4.

As can be seen from Table 4, the $mean\_S_{max}$ value is measured at a resolution of 5 Hz and when the flicker frequency is an integer multiple of 5 Hz, then the $mean\_S_{max}$ value is measured without an error, while it is measured with an error of 2% when the flicker frequency is not an integer multiple of 5 Hz (38/62 Hz or 938/962 Hz interharmonic). When working with a resolution of 0.5 Hz (2-s window length), $mean\_S_{max}$ is obtained without an error for all interharmonics. It may seem advantageous to work at a resolution of 0.5 Hz; however, as mentioned in [31], since the 2-s window length is too long for the power signal to be stationary, 5 Hz resolution (0.2-s window length) is preferred. Hence, in the rest of the study, 5 Hz resolution is used.

Table 4. Proposed VPD Flickermeter response for various sinusoidal voltage fluctuations.

	Voltage Fluctuation Required to Obtain $S_{max} = 1$ According to VPD Flickermeter		Proposed Flickermeter Response			
			5 Hz Resolution		0.5 Hz Resolution	
	f_{IH}, Hz	% $\frac{\Delta V}{V}$	$mean\_S_{max}$	% Error	$mean\_S_{max}$	% Error
In the case of a signal with a low frequency interharmonic	55/65	0.5125	1	0.00	1	0.00
	40/60	0.3505	1	0.00	1	0.00
	38/62	0.1565	1.02	2.00	1	0.00
	35/65	0.2182	1	0.00	1	0.00
	30/70	0.1300	1	0.00	1	0.00
	25/75	0.1971	1	0.00	1	0.00
In the case of a signal with a high interharmonic	955/965	0.5125	1	0.00	1	0.00
	940/960	0.3505	1	0.00	1	0.00
	938/962	0.1565	1.02	2.00	1	0.00
	935/965	0.2182	1	0.00	1	0.00
	930/970	0.1300	1	0.00	1	0.00
	925/975	0.1971	1	0.00	1	0.00

5.3. Response of the Proposed Flickermeter to the P_{st} Homogeneity Test

According to IEC standard, the response of flickermeter should be homogeneous; i.e., P_{st} is expected to increase proportional with the amplitude of the component causing the flicker [1]. To do this test, $\frac{\Delta V}{V}$ values in (6) are multipled with 0.5, 1 and 2 coefficients, respectively, and P_{st} values are computed. Tests are achieved for all amplitude values corresponding to the flicker frequencies (both low and high interharmonic frequencies) listed in Table 1 with 5-Hz resolution. The results of this study are given in Table 5.

Table 5. Response of proposed flickermeter to P_{st} homogeneity test.

f_{IH}	Response of Proposed Flickermeter to P_{st} Homogeneity Test/% Error			f_{IH}	Response of Proposed Flickermeter to P_{st} Homogeneity Test/% Error		
	$0.5\frac{\Delta V}{V}$	$\frac{\Delta V}{V}$	$2\frac{\Delta V}{V}$		$0.5\frac{\Delta V}{V}$	$\frac{\Delta V}{V}$	$2\frac{\Delta V}{V}$
25	0.3569/0.00	0.7139/0.00	1.4279/0.00	**925**	0.3569/0.00	0.7139/0.00	1.4279/0.00
30	0.3569/0.00	0.7139/0.00	1.4279/0.00	**930**	0.3569/0.00	0.7139/0.00	1.4278/0.00
32	0.4057/−0.01	0.8114/0.00	1.6232/+0.02	**932**	0.4057/−0.01	0.8113/0.00	1.6219/−0.04
35	0.3569/0.00	0.7139/0.00	1.4279/0.00	**935**	0.3569/0.00	0.7139/0.00	1.4279/0.00
38	0.3799/−0.07	0.7603/0.00	1.5206/0.00	**938**	0.3802/0.01	0.7603/0.00	1.5203/−0.02
40	0.3569/0.00	0.7139/0.00	1.4279/0.00	**940**	0.3569/0.00	0.7139/0.00	1.4280/0.00
45	0.3569/0.00	0.7139/0.00	1.4279/+0.01	**945**	0.3569/−0.01	0.7139/0.00	1.4280/+0.01
47.5	0.6504/−0.03	1.3011/0.00	2.6034/+0.04	**947.5**	0.6486/−0.21	1.2998/0.00	2.6095/+0.38
49.5	0.4801/−0.01	0.9603/0.00	1.9217/+0.06	**949.5**	0.4803/+0.03	0.9604/0.00	1.9229/+0.11
50.5	0.4801/−0.04	0.9605/0.00	1.9230/+0.11	**950.5**	0.4803/+0.02	0.9605/0.00	1.9234/+0.12
52.5	0.6505/−0.03	1.3014/0.00	2.6046/+0.07	**952.5**	0.6512/−0.13	1.3041/0.00	2.6143/+0.23
55	0.3569/0.00	0.7139/0.00	1.4279/+0.01	**955**	0.3569/0.00	0.7139/0.00	1.4280/+0.01
60	0.3569/0.00	0.7139/0.00	1.4279/+0.01	**960**	0.3569/0.00	0.7139/0.00	1.4278/0.00
62	0.3805/−0.01	0.7611/0.00	1.5224/+0.01	**962**	0.3806/−0.02	0.7613/0.00	1.5229/+0.02
65	0.3569/0.00	0.7139/0.00	1.4279/+0.01	**965**	0.3570/−0.01	0.7140/0.00	1.4283/+0.02
68	0.4061/−0.02	0.8123/0.00	1.6252/+0.04	**968**	0.4062/−0.04	0.8127/0.00	1.6258/+0.03
70	0.3569/0.00	0.7139/0.00	1.4279/+0.01	**970**	0.3570/−0.01	0.7140/0.00	1.4284/+0.02
75	0.3569/0.00	0.7139/0.00	1.4279/+0.01	**975**	0.3569/0.00	0.7139/0.00	1.4277/+0.00

As shown in Table 5, the proposed system produces outputs with a very low percentage error in the P_{st} homogeneity test, lower than 0.38% for all cases, while an error of 5% is allowed by the standard [1]. Especially considering that the DFT is applied for 5 Hz resolution, the results are very good for the flicker frequencies of 0.5, 2.5 and 12 Hz, which are not integer multiples of 5 Hz. It is also understood from the Table 5 that the situation for the high frequency interharmonics does not change.

5.4. Response of Proposed Flickermeter in Case the Signal Has a Flicker with 10 Hz Frequency and Relative Amplitude of $5\frac{\Delta V_{VPD}}{V}$ (Interharmonics at 40 Hz and 940 Hz)

The signals to be investigated are given in (48) and (49):

$$v(t) = V\left\{\sin(2\pi f t) + 5\frac{\Delta V_{VPD}}{V}\sin(2\pi 40 t)\right\}, \tag{48}$$

$$v(t) = V\left\{\sin(2\pi f t) + 5\frac{\Delta V_{VPD}}{V}\sin(2\pi 940 t)\right\}. \tag{49}$$

For these two signals with 40 Hz and 940 Hz interharmonics, i.e., 10 Hz flicker component, the maximum flicker sensation value $mean\_S_{max}$ is given in Table 6. The expected value of S is 25 in this case, since the square of S is shown to be directly proportional to the amplitude increase.

Table 6. Response of proposed flickermeter in the case of Equations (48) and (49).

	In the Case of a Signal with a 40 Hz Interharmonic		In the Case of a Signal with a 940 Hz Interharmonic	
f_{line}.Hz	$S_{1\ max}$	$S_{1\ max}$ % Error	$S_{1\ max}$	$S_{1\ max}$ % Error
49.5	25.10	0.40	25.10	0.40
49.6	25.08	0.32	25.08	0.32
49.7	25.07	0.28	25.07	0.28
49.8	25.05	0.20	25.05	0.20
49.9	25.03	0.12	25.03	0.12
50	25	1	25	0
50.1	24.97	−0.12	24.97	−0.12
50.2	24.93	−0.28	24.93	−0.28
50.3	24.89	−0.44	24.89	−0.44
50.4	24.86	−0.56	24.86	−0.56
50.5	24.82	−0.72	24.82	−0.72

As can be seen from Table 6, if the system frequency varies between 49.5 Hz and 50.5 Hz, the maximum error is 1.16%. The result is similar in the presence of 940 Hz components.

5.5. Response of Proposed Flickermeter in Case the Signal Has More Than One Flicker Component with Different Frequencies and Amplitudes

The signals used in this test are given in Equations (50) and (51) for both low- and high-frequency interharmonic components, and amplitudes are chosen from Table 1 so that unity S_{max} is expected at the output:

$$v(t) = V\left\{\sin(2\pi f t) + \begin{bmatrix} \frac{\Delta V_{VPD(45)}}{V}\sin(2\pi 45 t) + \frac{\Delta V_{VPD(40)}}{V}\sin(2\pi 40 t) \\ +\frac{\Delta V_{VPD(35)}}{V}\sin(2\pi 35 t)+ \\ \frac{\Delta V_{VPD(30)}}{V}\sin(2\pi 30 t) + \frac{\Delta V_{VPD(25)}}{V}\sin(2\pi 25 t) \end{bmatrix}\right\}, \tag{50}$$

$$v(t) = V\left\{\sin(2\pi f t) + \begin{bmatrix} \frac{\Delta V_{VPD(45)}}{V}\sin(2\pi 945 t) + \frac{\Delta V_{VPD(40)}}{V}\sin(2\pi 940 t) \\ +\frac{\Delta V_{VPD(35)}}{V}\sin(2\pi 935 t) \\ +\frac{\Delta V_{VPD(30)}}{V}\sin(2\pi 930 t) + \frac{\Delta V_{VPD(25)}}{V}\sin(2\pi 925 t) \end{bmatrix}\right\}. \tag{51}$$

For this test, the expected value of S is 5, since it has been shown previously that the effect of interharmonic components to the instantaneous flicker sensation S is additive [27]. The $mean\_S_{max}$ values obtained are given in Table 7 together with the corresponding error rates calculated as the deviation from 5.

Table 7. Response of proposed flickermeter in the case of Equations (50) and (51).

	In the Case of Interharmonics around the Fundamental Frequency		In the Case of Interharmonics around 950 Hz	
f_{line}.Hz	$S_{1\ max}$	$S_{1\ max}$ % Error	$S_{1\ max}$	$S_{1\ max}$ % Error
49.5	5.20	4.0	5.29	5.80
49.6	5.12	2.4	5.28	5.60
49.7	5.07	1.4	5.05	1.00
49.8	5.03	0.6	5	0
49.9	5.01	0.2	5.03	0.60
50	5	1	5	0
50.1	5	1	5.04	0.80
50.2	5.02	0.4	5.03	0.60
50.3	5.05	1.0	5.10	2.00
50.4	5.09	1.8	5.26	5.20
50.5	5.15	3.0	5.29	5.80

It is clear that, if the fundamental frequency is increased or decreased, $mean\_S_{max}$ is obtained by the S1 method with a maximum of 4% error if there is an interharmonic component around the fundamental harmonic. In the presence of interharmonics around 950 Hz, the error may exceed 5%; however, for the cases of frequency deviation more than ±0.3 Hz. On the other hand, as mentioned in [27], new generation systems usually have maximum frequency shifts of ±0.2 Hz and when this frequency deviation range is taken into consideration, an error below 1% is obtained.

5.6. Response of Proposed Flickermeter in Case the Signal Has More Than One Flicker Component with Different Frequencies and Different Amplitudes

The signals used in this test are given in Equations (52) and (53) for both low- and high-frequency interharmonic components, and different multiples of amplitudes are chosen from Table 1 so that S is expected to be 55 (summation of the square of each multiple) at the output:

$$v(t) = V\left\{\sin(2\pi f t) + \begin{bmatrix} 5\frac{\Delta V_{VPD(45)}}{V}\sin(2\pi 45t) + 4\frac{\Delta V_{VPD(40)}}{V}\sin(2\pi 40t) \\ +3\frac{\Delta V_{VPD(35)}}{V}\sin(2\pi 35t) \\ +2\frac{\Delta V_{VPD(30)}}{V}\sin(2\pi 30t) + \frac{\Delta V_{VPD(25)}}{V}\sin(2\pi 25t) \end{bmatrix}\right\}, \tag{52}$$

$$v(t) = V\left\{\sin(2\pi f t) + \begin{bmatrix} 5\frac{\Delta V_{VPD(45)}}{V}\sin(2\pi 945t) + 4\frac{\Delta V_{VPD(40)}}{V}\sin(2\pi 940t) \\ +3\frac{\Delta V_{VPD(35)}}{V}\sin(2\pi 935t) \\ +2\frac{\Delta V_{VPD(30)}}{V}\sin(2\pi 930t) + \frac{\Delta V_{VPD(25)}}{V}\sin(2\pi 925t) \end{bmatrix}\right\}. \tag{53}$$

For this test, the $mean\_S_{max}$ is given in Table 8 together with the error rates calculated based on the expected result, which is 55.

6. Proposed VPD Flickermeter Response to Field Data

The field data used in this work has been obtained from the electricity transmission system of Turkey by the power quality monitoring devices developed through the National Power Quality Project of Turkey [32]. The data has been collected from a transformer substation supplying an electric arc furnace (EAF) plant; therefore, it is rich in highly time-varying interharmonics and hence suffers from significant flicker. It is 10-min data collected from three different phases simultaneously at a sampling frequency of 3.2 KHz.

Table 8. Response of proposed flickermeter in the case of Equations (52) and (53).

	In the Case of Interharmonics around the Fundamental Frequency		In the Case of Interharmonics around 950 Hz	
$\mathbf{f_{line}}$.**Hz**	$S_{1\ max}$	$S_{1\ max}$ **% Error**	$\mathbf{f_{line}}$.**Hz**	$S_{1\ max}$
49.5	56.89	3.4	57.41	4.38
49.6	56.44	2.6	58.73	6.78
49.7	56.03	1.87	54.56	−0.80
49.8	55.64	1.17	54.85	−0.27
49.9	55.30	0.55	55.61	1.11
50	55.06	0.11	55.04	0.07
50.1	54.77	0.42	55.50	0.91
50.2	54.59	0.75	54.69	−0.56
50.3	54.50	0.91	56.01	1.84
50.4	54.52	0.88	58.16	5.75
50.5	54.64	0.65	56.27	2.31

For all phases of the collected voltage waveform, frequency variation is calculated. In addition, instantaneous flicker sensation values ($mean\_S_{max}$) for 10 min are obtained using the proposed method, the IEC flickermeter and the flickermeter proposed in [27], which does not consider the high-frequency flicker components. All results are plotted together in Figures 3–5 for both the whole 10-min measurement period and also for a sample 1-min period to observe the details for comparison purposes.

S_{max} values are calculated for 0.2-s (10 cycle of the fundamental) windows overlapping 9-cycles, hence generating one S_{max} value every cycle and average of each 10-cycle is taken to obtain one S value at each 0.2-s window. The averages have been calculated by using the S_1 method considering the simplified IEC flickermeter [27] and the proposed VPD flickermeter.

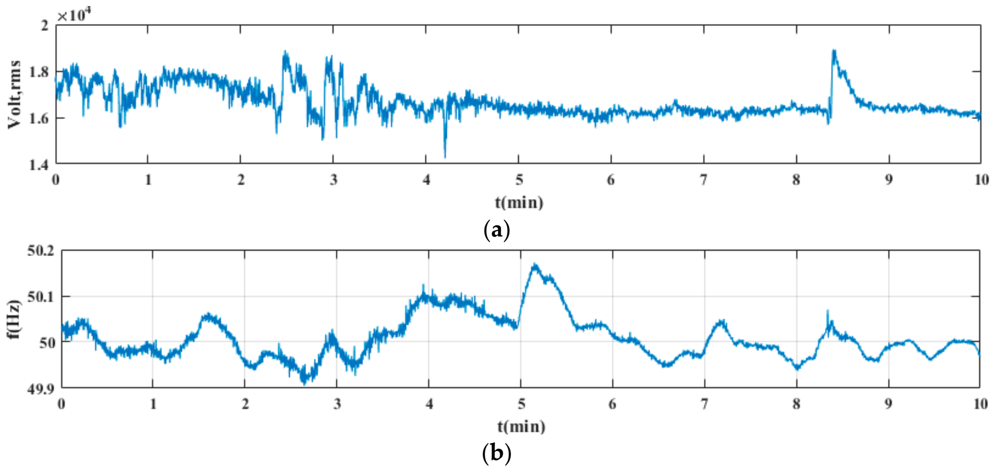

Figure 3. *Cont.*

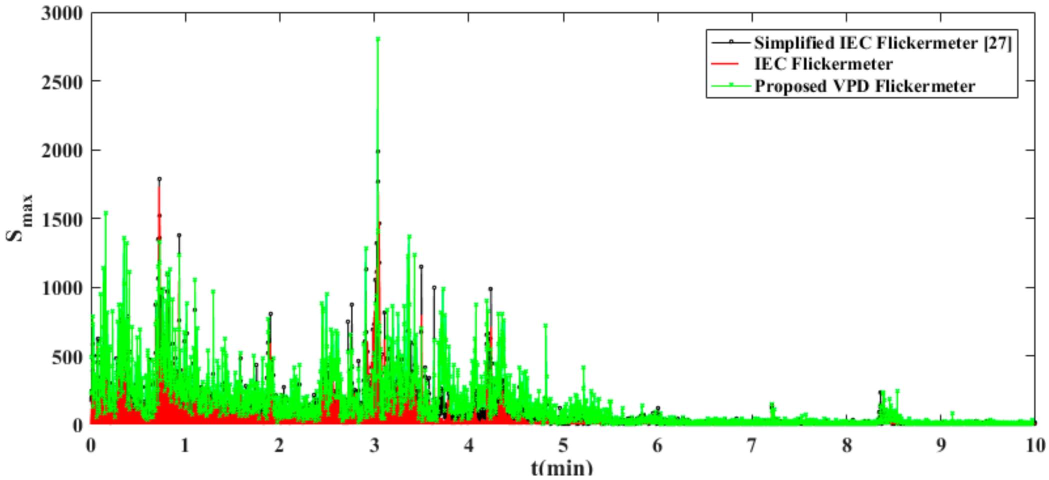

(**c**)

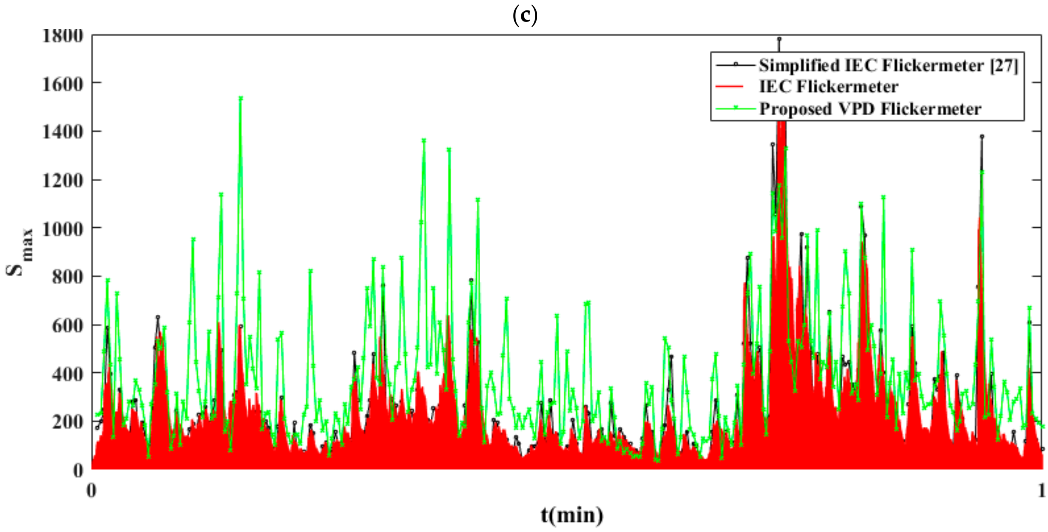

(**d**)

Figure 3. Evaluations for phase 1 (**a**) RMS variation; (**b**) fundamental frequency variation; (**c**) comparison of 10 min S_{max} for different methods; (**d**) comparison of 1 min zoomed version of S_{max} for different methods.

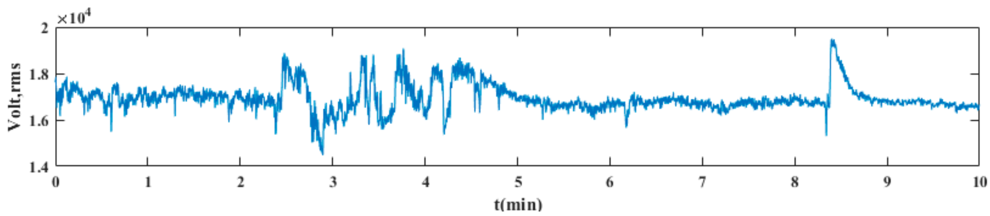

(**a**)

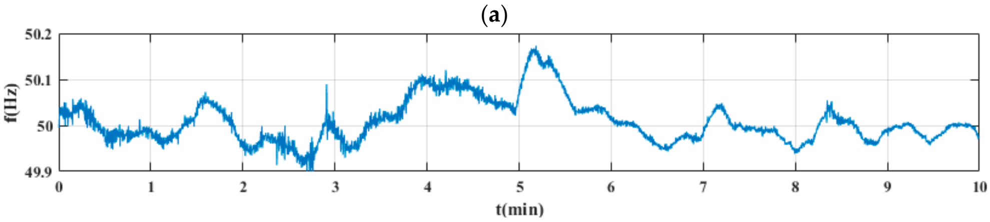

(**b**)

Figure 4. *Cont.*

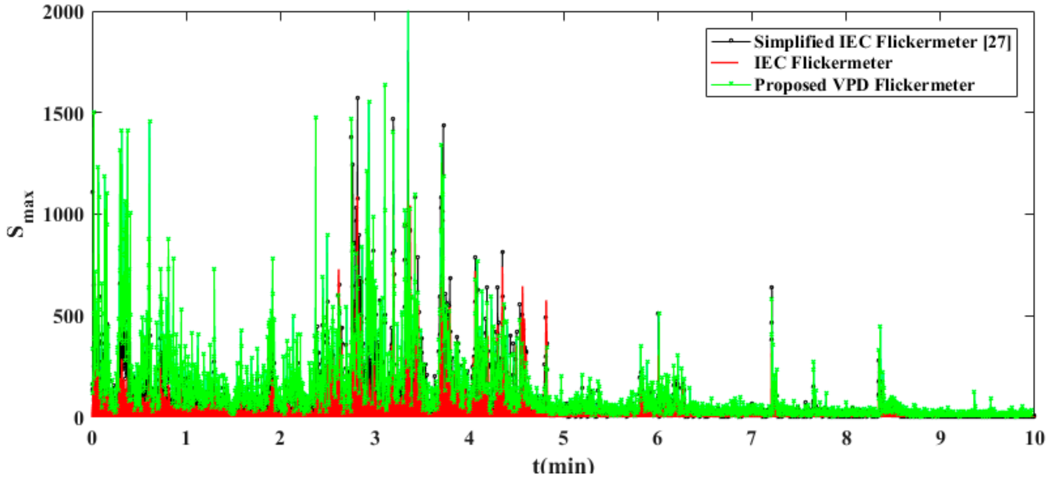

(**c**)

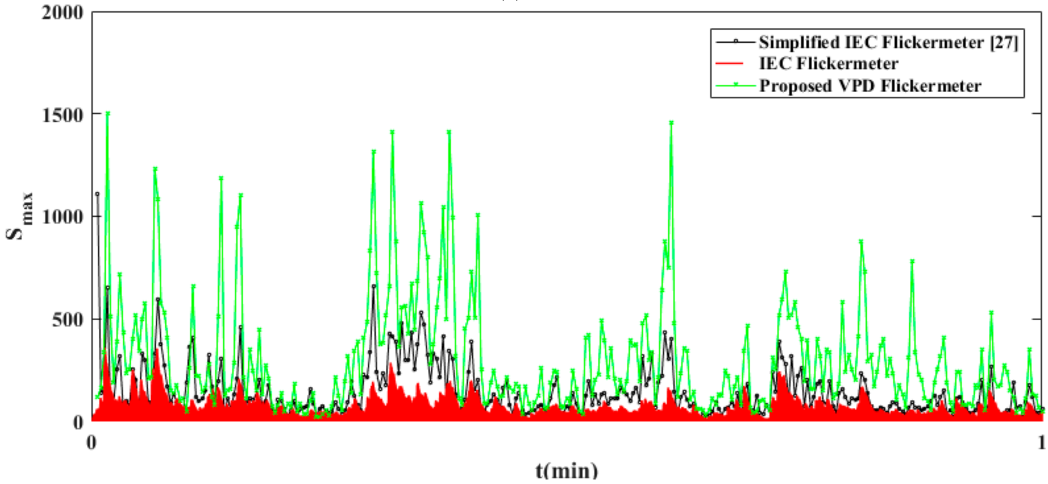

(**d**)

Figure 4. Evaluations for phase 2 (**a**) RMS variation; (**b**) fundamental frequency variation; (**c**) comparison of 10 min S_{max} for different methods; (**d**) comparison of 1 min zoomed version of S_{max} for different methods.

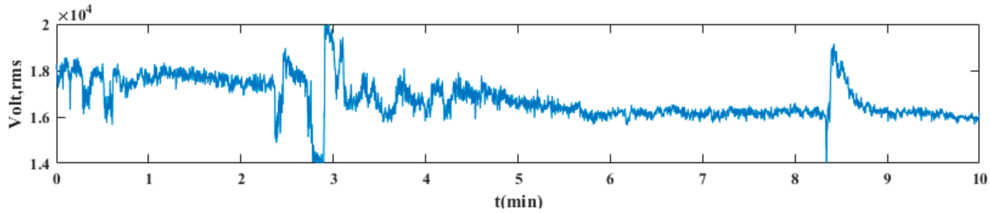

(**a**)

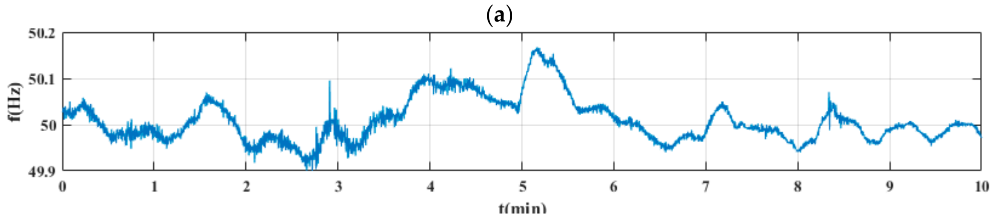

(**b**)

Figure 5. *Cont.*

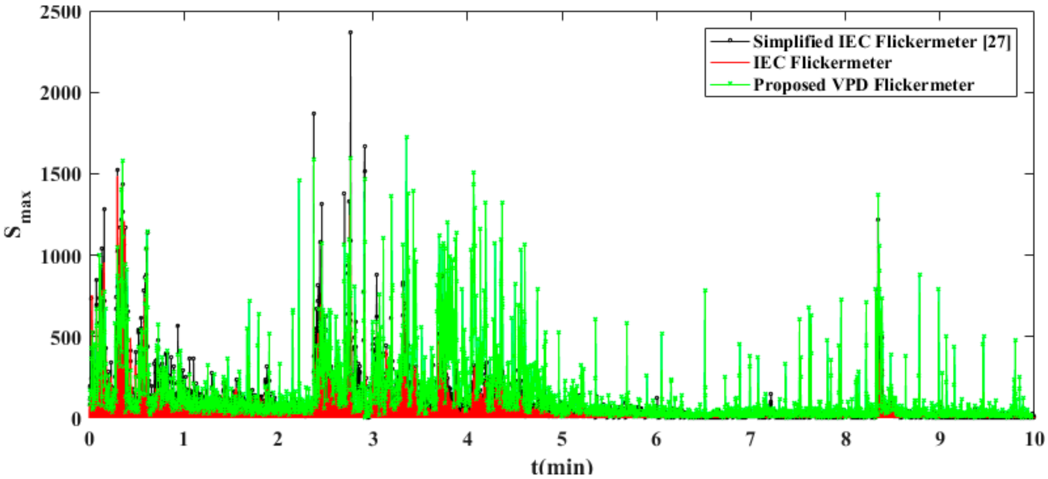

(**c**)

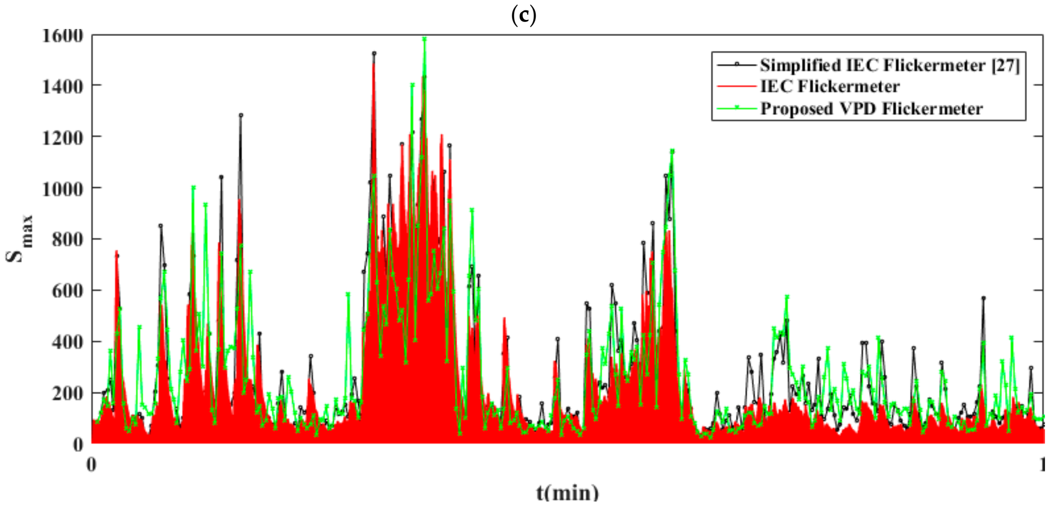

(**d**)

Figure 5. Evaluations for phase 3 (**a**) RMS variation; (**b**) fundamental frequency variation; (**c**) comparison of 10 min S_{max} for different methods; (**d**) comparison of 1 min zoomed version of S_{max} for different methods.

It is observed in Figures 3–5 that the results of the IEC flickermeter and the simplified IEC flickermeter are very close to each other. This shows that the results obtained by the S_1 method using the method of [27] are consistent with the results obtained from the IEC flickermeter. However, as can be seen from the tests, using synthetic data that the flicker produced by the high frequency components cannot be detected. In addition, to the knowledge of the authors, there is no work in the literature to determine the effect of the high-frequency interharmonics when the fundamental frequency is deviating. It is seen that the S_{max} results obtained with the proposed VPD flickermeter have similar tendencies of increase and decrease with the results of the IEC flickermeter and the simplified IEC flickermeter in [27]. The differences can be interpreted as the effect of the high-frequency components detected by the proposed VPD flickermeter, which can't be detected with the IEC flickermeter and the simplified IEC flickermeter in [27]. For this reason, the values of S_{max} and P_{st} obtained with the VPD flickermeter are usually somewhat higher.

Table 9 shows the P_{st} values obtained for the three different flickermeters used. In a similar manner, higher P_{st} values are obtained because the proposed VPD flickermeter senses the flicker caused by the high frequency interharmonic components.

Table 9. P_{st} values of each phase for different methods.

Phase/Method	IEC 61000-4-15 Flickermeter	Simplified IEC Flickermeter [27]	Proposed VPD Flickermeter
Phase 1	13.9669	13.5818	15.6923
Phase 2	12.5231	13.6565	15.3588
Phase 3	13.4152	14.0900	16.4933

7. Conclusions

In this article, a flickermeter developed based on the voltage-peak-detection (VPD) flickermeter, which is more robust to fundamental frequency deviations, is presented. The maximum value of the instantaneous flicker sensation, S_{max}, obtained from the VPD flickermeter has been shown to be approximately equal to the sum of the squares of the amplitudes of the flicker generating frequency components. With this representation, a simplified VPD flickermeter has been developed with the help of the VPD flicker curve. Satisfactory results are revealed from the tests using this new flickermeter made with synthetically produced voltage signals with both low and high frequency interharmonic components. Comparison of the results with the results of the IEC flickermeter and a simplified flickermeter proposed in [27] has shown that the proposed flickermeter provides more robust results in cases of fundamental frequency deviations, which is a common and contemporary problem of the electricity transmission or distribution systems with highly time-varying loads and renewable energy sources. In the field data tests, the standard IEC flickermeter produced S_{max} values less than those produced by the proposed VPD-based method, which is a natural result because the proposed method considers the effect of the high frequency interharmonic components on the flicker sensation. When the short-term flicker severity, P_{st}, values are considered, the situation is also similar. Considering all of these results and the literature survey, it can be concluded that there exists no effective flickermeter, which takes care of both the high frequency interharmonic components and is robust to the fundamental frequency changes in the literature. Hence, an efficient and usable VPD-based flickermeter is proposed.

Author Contributions: S.A. and Ö.S. proposed the methodology. S.A. improved the method and performed the simulations and wrote the manuscript. Both authors reviewed and polished the manuscript.

Acknowledgments: The field data used in this article were obtained within the scope of the Power Quality National Project. The authors would like to thank the TUBITAK-KAMAG group.

Conflicts of Interest: The authors declare no conflict of interest.

References

1. IEC. *Electromagnetic Compatibility (EMC) Part 4–15: Testing and Measurement Techniques Flickermeter Functional and Design Specifications*; IEC 61000-4-15; IEC: Geneva, Switzerland, 2011.
2. Zargari, A.; Moallem, P.; Kiyoumarsi, A. Studying and improvement of operation of IEC flickermeter. In Proceedings of the ICEE 2010 18th Iranian Conference on Electrical Engineering, Isfahan, Iran, 11–13 May 2010; pp. 925–931.
3. Silsupur, M.; Turkay, B.E. Flicker source detection methods based on IEC 61000-4-15 and signal processing techniques—A review. *Balk. J. Electr. Comput. Eng.* **2015**, *3*, 93–97.
4. Gutierrez, J.J.; Azcarate, I.; Saiz, P.; Lazkano, A.; Leturiondo, L.A.; Redondo, K. An alternative strategy to improve the flicker severity measurement. *Int. J. Electr. Power Energy Syst.* **2014**, *63*, 667–673. [CrossRef]
5. Gutierrez, J.J.; Saiz, P.; Leturiondo, L.A.; Azcarate, I.; Redondo, K.; Lazkano, A. Flicker measurement in real scenarios: Reducing the divergence from the human perception. *Electr. Power Syst. Res.* **2016**, *140*, 312–320. [CrossRef]
6. Azcarate, I.; Gutierrez, J.J.; Saiz, P.; Lazkano, A.; Leturiondo, L.A.; Redondo, K. Flicker characteristics of efficient lighting assessed by the IEC flickermeter. *Electr. Power Syst. Res.* **2014**, *107*, 21–27. [CrossRef]
7. Azcarate, I.; Gutierrez, J.J.; Lazkano, A.; Saiz, P.; Redondo, K.; Leturiondo, L.A. Experimental study of the response of efficient lighting technologies to complex voltage fluctuations. *Int. J. Electr. Power Energy Syst.* **2014**, *63*, 499–506. [CrossRef]

8. Turkuzan, M.; Salor, O. Illumination based flickermeter designed for flicker analysis of electric arc furnace plants. In Proceedings of the 2016 52nd Annual Meeting of the IEEE Industry Applications Society (IAS), Portland, OR, USA, 2–6 October 2016; pp. 1–8.
9. Gil-de-Castro, A.; Ronnberg, S.K.; Bonen, M.H.J. Light intensity variation (flicker) and harmonic emission related to led lamps. *Electr. Power Syst. Res.* **2017**, *146*, 107–114. [CrossRef]
10. Gutierrez, J.J.; Saiz, P.; Azcarate, I.; Leturiondo, L.A.; Redondo, K.; de Gauna, S.R.; Gonzalez-Otero, D.M. Sensitivity of modern lighting technologies at varying flicker severity levels. *Int. J. Electr. Power Energy Syst.* **2017**, *92*, 34–41. [CrossRef]
11. Chang, G.W.; Lu, H.J.; Chuang, C.S. An accurate hybrid intelligent approach for forecasting flicker severity caused by electric arc furnaces. *Electr. Power Syst. Res.* **2015**, *121*, 101–108. [CrossRef]
12. Wiczynski, G. Estimation of pst indicator value for a simultaneous influence of two disturbing loads. *Electr. Power Syst. Res.* **2017**, *147*, 97–104. [CrossRef]
13. Athira, S.; Harikumar, K.; Soman, K.P.; Poornachandran, P. An optimization algorithm for voltage flicker analysis. *Procedia Technol.* **2015**, *21*, 589–595. [CrossRef]
14. Chen, C.I.; Chen, Y.C.; Chang, Y.R.; Lee, Y.D. An accurate solution procedure for calculation of voltage flicker components. *IEEE Trans. Ind. Electr.* **2014**, *61*, 2370–2377. [CrossRef]
15. Goh, Z.P.; Radzi, M.A.M.; Hizam, H.; Wahab, N.I.A. Investigation of severity of voltage flicker caused by second harmonic. *IET Sci. Meas. Technol.* **2017**, *11*, 363–370. [CrossRef]
16. Xu, W.L. Deficiency of the IEC flicker meter for measuring interharmonic-caused voltage flickers. In Proceedings of the 2005 IEEE Power Engineering Society General Meeting, San Francisco, CA, USA, 16 June 2005; pp. 2326–2329.
17. Koponen, P.; Hansen, H.; Bollen, M. Interharmonics and light flicker. In Proceedings of the 23rd International Conference on Electricity Distribution, Lyon, France, 15–18 June 2015; p. 1100.
18. SlezIngr, J.; Drapela, J. An alternative flickermeter evaluating high-frequency interharmonic voltages. In Proceedings of the IEEE 2012 International Workshop on Applied Measurements for Power Systems (AMPS) Proceedings, Aachen, Germany, 26–28 September 2012; pp. 1–6.
19. Hooshyar, A.; El-Saadany, E.F. Development of a flickermeter to measure non-incandescent lamps flicker. *IEEE Trans. Power Deliv.* **2013**, *28*, 2103–2115. [CrossRef]
20. Tayjasanant, T.; Wang, W.C.; Li, C.; Xu, W.S. Interharmonic-flicker curves. *IEEE Trans. Power Deliv.* **2005**, *20*, 1017–1024. [CrossRef]
21. Kim, T.; Rylander, M.; Powers, E.J.; Grady, W.M.; Arapostathis, A. Led lamp flicker caused by interharmonics. In Proceedings of the 2008 IEEE Instrumentation and Measurement Technology Conference, Victoria, BC, Canada, 12–15 May 2008; pp. 1920–1925.
22. Drapela, J.; Toman, P. Interharmonic-flicker curves of lamps and compatibility level for interharmonic voltages. In Proceedings of the 2007 IEEE Lausanne Powertech, Lausanne, Switzerland, 1–5 July 2007; pp. 1552–1557.
23. Koster, M.D.; Jaiger, E.D.; Vancoistem, W. Light Flicker Caused by Interharmonics. Available online: http://grouper.ieee.org/groups/harmonic/iharm/ihflicker.pdf (accessed on 8 February 2018).
24. Drapela, J. A time domain based flickermeter with response to high frequency interharmonics. In Proceedings of the 2008 13th International Conference on Harmonics and Quality of Power, Wollongong, Australia, 28 September–1 October 2008; pp. 154–160.
25. Kim, T.; Wang, A.; Powers, E.J.; Grady, W.M.; Arapostathis, A. Detection of flicker caused by high-frequency interharmonics. In Proceedings of the 2007 IEEE Instrumentation & Measurement Technology Conference, Warsaw, Poland, 1–3 May 2007; pp. 1–5.
26. Kim, T.; Powers, E.J.; Grady, W.M.; Arapostathis, A. Detection of flicker caused by interharmonics. *IEEE Trans. Instrum. Meas.* **2009**, *58*, 152–160.
27. Kose, N.; Salor, O. New spectral decomposition based approach for flicker evaluation of electric arc furnaces. *IET Gener. Trans. Distrib.* **2009**, *3*, 393–411. [CrossRef]
28. Akkaya, S.; Salor, O. Flicker detection algorithm based on the whole voltage frequency spectrum for new generation lamps: Enhanced VPD flickermeter model & flicker curve. *IET Sci. Meas. Technol.* **2017**. Submitted.

29. Duric, M.B.; Durisic, Z.R. Frequency measurement in power networks in the presence of harmonics using fourier and zero crossing technique. In Proceedings of the IEEE Russia Power Tech, St. Petersburg, Russia, 27–30 June 2005; pp. 1–6.
30. Salor, O. Spectral correction based method for interharmonics analysis of power signals with fundamental frequency deviation. *Electr. Power Syst. Res.* **2009**, *79*, 1025–1031. [CrossRef]
31. IEC. *IEC Standard 61000-4-7: General Guide on Harmonics and Interharmonics Measurements and Measuring Instruments for Power Supply Networks and Attached Devices Used for the Measurements*; IEC: Geneva, Switzerland, 2009.
32. Demirci, T.; Kalaycioglu, A.; Kucuk, D.; Salor, O.; Guderl, M.; Pakhuylu, S.; Atalik, T.; Inan, T.; Cadirci, I.; Akkaya, Y.; et al. Nationwide real-time monitoring system for electrical quantities and power quality of the electricity transmission system. *IET Gener. Trans. Distrib.* **2011**, *5*, 540–550. [CrossRef]